



Characteristics of High Saturation Hydrate Reservoirs in the Low-Angle Subduction Area of the Makran Accretionary Prism

Jing Liao^{1,2}, Xinxin Liu^{1,2}, Qingfang Zhao^{1,2*}, Jianming Gong^{1,2}, Weihan Yin^{3,4}, Sen Li^{1,2}, Baohua Lei^{1,2}, Jie Liang^{1,2}, Khalid Muhammad⁵ and Waseem Haider Syed⁶

¹Qingdao Institute of Marine Geology, China Geological Survey, Qingdao, China, ²Laboratory for Marine Mineral Resources, Pilot National Laboratory for Marine Science and Technology, Qingdao, China, ³North China Sea Environmental Monitoring Center, SOA, Qingdao, China, ⁴Key Laboratory of Ecological Prewarning, Protection and Restoration of Bohai Sea, MNR, Qingdao, China, ⁵Pakistan Hydrographic Department, Liaquat Barracks Shahrae Faisal, Karachi, Pakistan, ⁶National Institute of Oceanography, Karachi, Pakistan

OPEN ACCESS

Edited by:

Pibo Su,
Guangzhou Marine Geological Survey,
China

Reviewed by:

Zhenquan Lu,
China Geological Survey, China
Jiasheng Wang,
China University of Geosciences
Wuhan, China
Xin Su,
China University of Geosciences,
China

*Correspondence:

Qingfang Zhao
zqingfang@mail.cgs.gov.cn

Specialty section:

This article was submitted to
Marine Geoscience,
a section of the journal
Frontiers in Earth Science

Received: 24 January 2022

Accepted: 28 March 2022

Published: 26 April 2022

Citation:

Liao J, Liu X, Zhao Q, Gong J, Yin W,
Li S, Lei B, Liang J, Muhammad K and
Syed WH (2022) Characteristics of
High Saturation Hydrate Reservoirs in
the Low-Angle Subduction Area of the
Makran Accretionary Prism.
Front. Earth Sci. 10:861162.
doi: 10.3389/feart.2022.861162

To delineate the spatial distribution of high saturation gas hydrate reservoirs in the low-angle subduction areas of the Makran Accretionary Prism, we conducted seismic data interpretation and impedance inversion of gas hydrates in the Makran Accretionary Prism and comprehensively analyzed the characteristics of the high saturation gas hydrate reservoirs in the Nankai Trough in Japan and the Shenhu Area in the South China Sea. The results show that the Makran Accretionary Prism features thick sediments, developed transport systems of “two-way gas supply” (i.e., thrust fault and normal fault, thrust fault and high permeable strata), and clear and continuous bottom simulating reflector (BSR). Meanwhile, strong-amplitude reflectors and strong-impedance anomalies coexist in the anticline wing above the BSR. Combined with the proven characteristics of high saturation gas hydrate reservoir, the high saturation gas hydrate reservoirs in the Makran Accretionary Prism are probably mainly distributed in the anticline wings immediately above the BSR. These results provide useful information for the exploration and development of gas hydrate in the low-angle subduction area of the Makran Accretionary Prism.

Keywords: high saturation hydrate deposit, reservoir characteristic comparison, impedance anomalies, low-angle subduction area, Makran Accretionary Prism

1 GEOLOGICAL SETTING

At present, the accumulation mechanism of gas hydrate in the high-angle subduction area of the active continental margin is relatively clear (Hyndman and Spence, 1992; Baba and Yamada, 2004; Zhang et al., 2006; Riedel et al., 2010; Hu et al., 2020), however the accumulation mechanism of gas hydrate in the low-angle subduction area is rarely reported (Gong et al., 2018a). Makran Accretionary Prism is located in the active continental margin with the lowest subduction angle worldwide, in which has complex thrust structure and widely distributed BSRs in the slope area, indicating that gas hydrate has a great potential in this area. Therefore, Makran Accretionary Prism can be viewed as a natural laboratory to study hydrate accumulation mechanisms in the low-angle subduction margins.

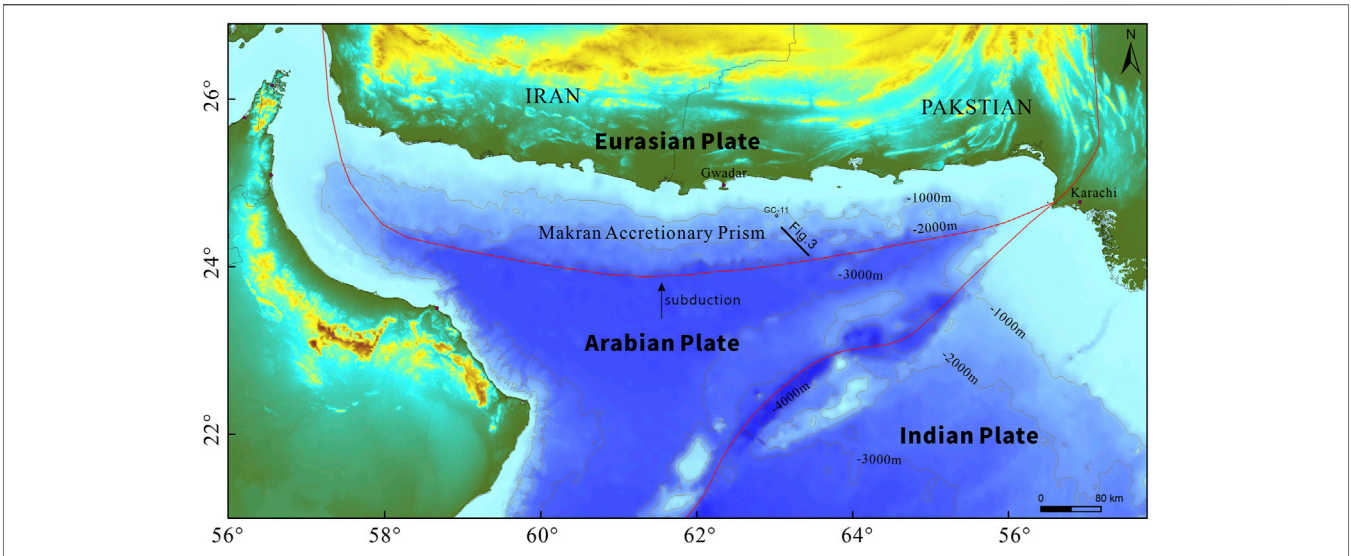


FIGURE 1 | Locations of the study area and seismic profile.

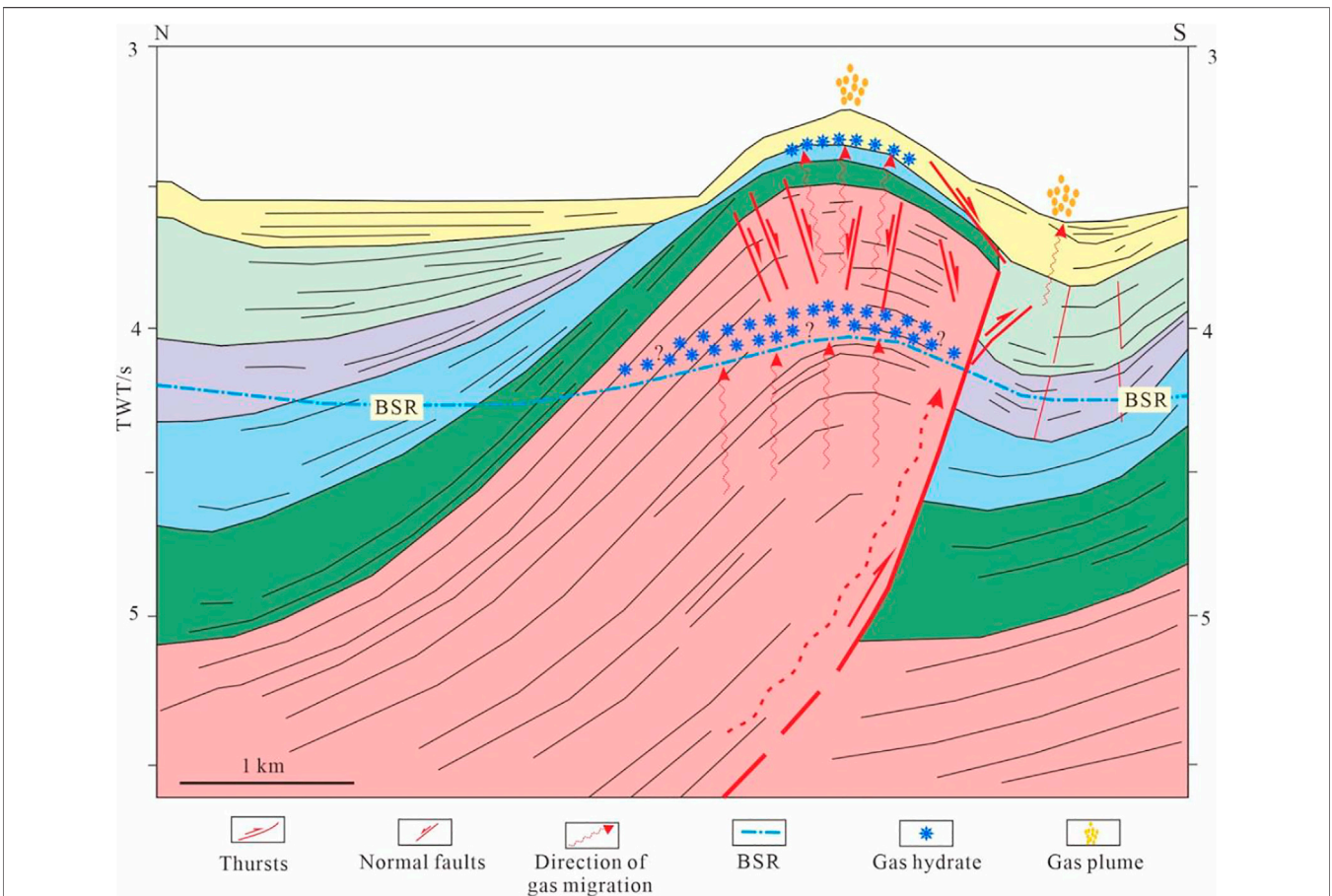
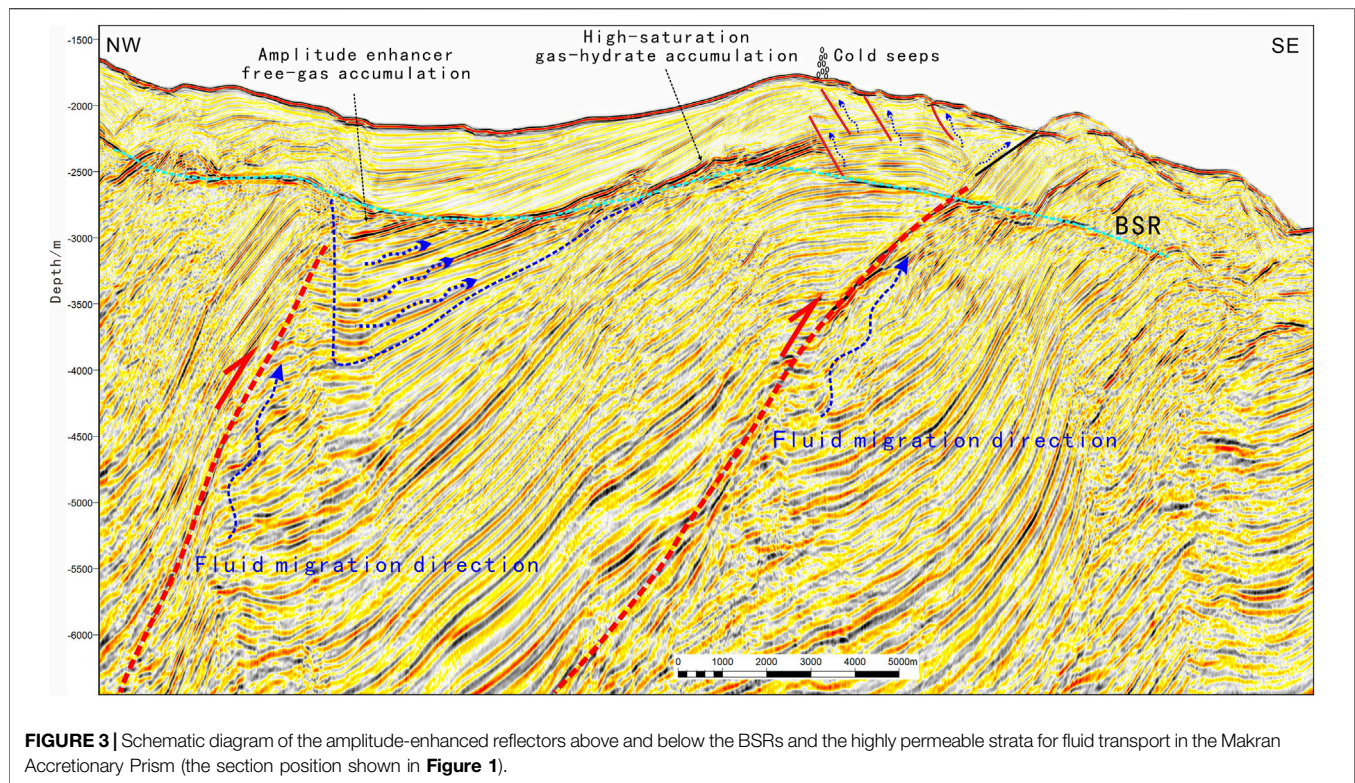


FIGURE 2 | Gas hydrate accumulation model of a two-story structure in the Makran Accretionary Prism (modified after Grando and McCla, 2007; Gong et al., 2018a).



The Makran Accretionary Prism in the northwest Indian Ocean was formed by the low-angle subduction of the Arabian Plate beneath the Eurasian Plate (**Figure 1**) Owing to the low subduction angle (less than 3°) and abundant sediments from the Eurasian Plate, the sediments of the Makran Accretionary Prism are over 7,000 m thick (Kopp et al., 2000; Grando and McClain, 2007). These sediments serve as the source rock for the formation of gas hydrates in the area. According to drilling and seismic data, the Makran Accretionary Prism is mainly composed of Cenozoic strata (Hussain et al., 2015; Gong et al., 2018b). Our findings suggest that Paleogene abyssal-facies mudstones and Miocene bathyal-facies mudstones are primary source rocks of gas hydrates in this area. According to the calculations using temperature and pressure fields under which gas hydrates remain stable, the gas hydrates in the Makran Accretionary Prism have developed in areas with a water depth of over 800 m, and distributed in sediments 300–700 m below the seafloor. The sediments are Pliocene-Quaternary strata and primarily consist of pelagic and hemipelagic mudstones interbedded with turbidites.

During surveys of several cruises in 1997, 1998 and 2007 (SO-122, SO-123, SO-124, SO-130 and (M74/3), gas seepage and a number of microbial mats were found (Von Rad et al., 2000). Previous studies have identified the distribution of BSR from 2D seismic data offshore Makran (Von Rad et al., 2000; Grevenmeyer et al., 2000; Smith, 2013; Liao et al., 2019). Full wave-form inversion suggests that gas hydrate concentrations above the

BSR as low as 10%, and most free-gas below BSR (Sain et al., 2000). Hydrate samples are porous and tubular, cold springs and plumes highly rise (Bohrmann and Ohling, 2008). Meanwhile, burnable methane is spewed out of near-shore mud volcanoes (Von Rad et al., 2000; Delisle et al., 2002, 2004; Zhang et al., 2020). Therefore, the Makran Accretionary Prism has sufficient gas sources and favorable accumulation conditions for gas hydrates. Compared with other active continental margins, Makran Accretionary Prism has thicker free gas under the BSR (Sain et al., 2000; Smith, 2013). According to seismic data interpretation, fluids are mainly transported by deep thrust faults and highly permeable strata, followed by superficial small normal faults, and gas hydrates are mainly distributed in seafloor surface anticlinal ridges and strata immediately above the BSR (**Figure 2**) (Gong et al., 2016; Gong et al., 2018b).

2 DATA AND METHODOLOGY

2.1 Data Acquisition

The seismic data acquired in late 2019. Due to the increase of the record time and length of seismic cable (**Supplementary Table S1**), the resolution of seismic data has been greatly improved. This study incorporates the seismic and logging data from gas hydrate drilling holes in the Nankai Trough, Japan and the Shenhu Area, South China Sea to compare the characteristics of high saturation gas hydrate reservoirs by impedance inversion.

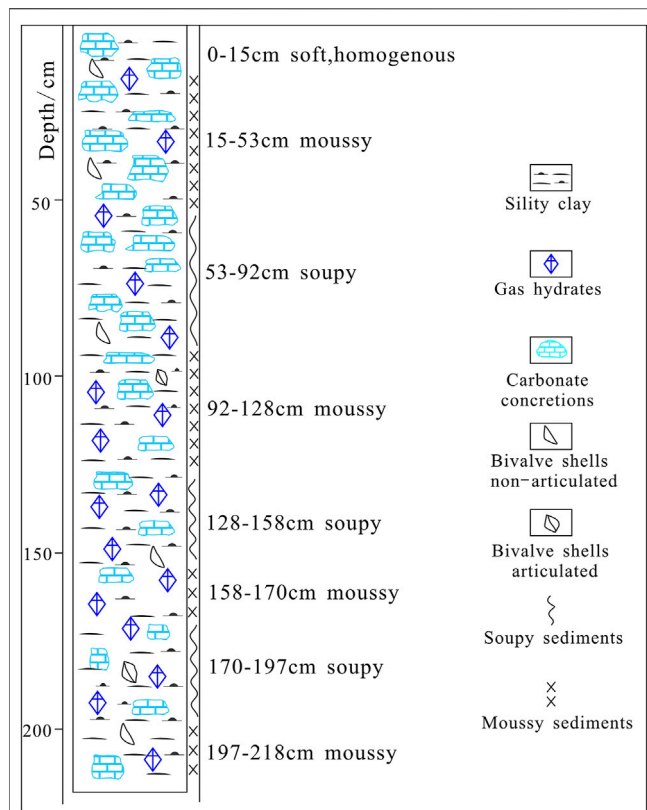


FIGURE 4 | Gravity core GC-11 from the Makran Accretionary Prism shows sporadically distributed hydrates in silty clay (Modified after Bohrmann and Ohling, 2008; Gong et al., 2017, site position shown in **Figure 1**).

2.2 Methodology

2.2.1 Seismic Interpretation and Impedance Inversion

Synthetic seismic records of gas hydrate-bearing layers were obtained using the reflection characteristics of seismic wave groups (i.e., external geometrical morphology, internal reflection structure, continuity, amplitude, frequency, and layer velocity), as well as regional geological data. Gas hydrate-bearing strata generally show strong amplitude anomalies in the synthetic seismic records (Riedel et al., 2010). Seismic impedance can well reflect the characteristics of gas hydrates (such as BSRs), and the applications of wave impedance in the identification of gas hydrate and the study of the concentration assessments have achieved good results (Riedel and Shankar, 2012; Wan et al., 2016; Xue et al., 2016; Li et al., 2019). In this study on the characteristics of hydrate-bearing reservoirs, we performed well-free acoustic impedance inversion using seismic data because there is no logging data in the study area. The low-frequency impedance model was obtained by seismic velocity data.

Most of the strata at the target location have large dip angle, which imposes higher requirements for the low-frequency model. It is necessary to improve the accuracy of seismic interpretation in the early stage to ensure the accuracy of horizon information. In order to ensure the rationality of the low-frequency impedance model, we extracted wavelets at multiple locations and obtained the optimal wavelet. Then, we used the inversion results to correct the initial

model iteratively and finally obtained the final impedance inversion results. The high saturation hydrate reservoirs on the impedance inversion profile can be characterized by high impedance anomalies.

2.2.2 Hydrate Reservoir Correlation

A comparative analysis was conducted on the characteristics (e.g., lithology, thickness, and sedimentary facies) of high saturation hydrate layers using the seismic and logging data of high saturation hydrate concentrated areas confirmed by drilling in Nankai Trough and Shenhu area in South China Sea. In this way, the characteristics of the seismic reflections and inversed impedance anomalies of high saturation hydrate concentrated areas were determined. Based on this information, the authors can predict high saturation hydrate concentrated zones in the Makran Accretionary Prism.

3 RESULTS AND DISCUSSION

3.1 Seismic Interpretation and Impedance Inversion of the Makran Accretionary Prism

3.1.1 Amplitude-Enhanced Reflectors

According to the interpretation of newly acquired high-resolution seismic data, the BSR in the study area shows noticeable reflection characteristics and is continuously distributed, and fluids are transported by massive highly permeable strata (indicated with blue arrows in **Figure 3**) as well as deep thrust faults and shallow normal faults. Most of the highly permeable strata are located in the piggyback basin under the BSR. They correspond to the negative topography of the seafloor and are present as inclined amplitude-enhanced reflectors in the seismic profile (**Figure 3**). As revealed by previous studies, the amplitude-enhanced reflectors above the BSR are generally the high saturation hydrate concentrated zones (Guo et al., 2017), whereas those below the BSR are usually free gas concentrated zones (Riedel et al., 2010). Analysis shows that the free gas layers under the BSR in the Makran Accretionary Prism are 200–300 m thick (Grevenmeyer et al., 2000; Sain et al., 2000; Ojha and Sain, 2008), indicating that the Makran Accretionary Prism has abundant gas sources. However, there are no apparent amplitude-enhanced reflectors in the shallow depth strata near seafloor of the Makran Accretionary Prism. This may be related to the small particle size of surface sediments (mainly including silty clay) and the low saturation hydrates with sporadic distribution (**Figure 4**) (Bohrmann and Ohling, 2008; Gong et al., 2017).

3.1.2 Impedance Inversion

Seismic data interpretation has revealed that the gas hydrates in the Makran Accretionary Prism are mainly concentrated in the anticlinal ridge and have a two-story structure (Gong et al., 2016; Gong et al., 2018a). To date, surface hydrate samples have been obtained from gravity cores (**Figure 4**), but the deep hydrate layers close to the BSR have not been drilled. Shallow hydrate-bearing sediments show weak amplitude or blank reflections in the seismic profile (**Figure 3**). By contrast, the unconfirmed deep hydrate layers above the BSR are

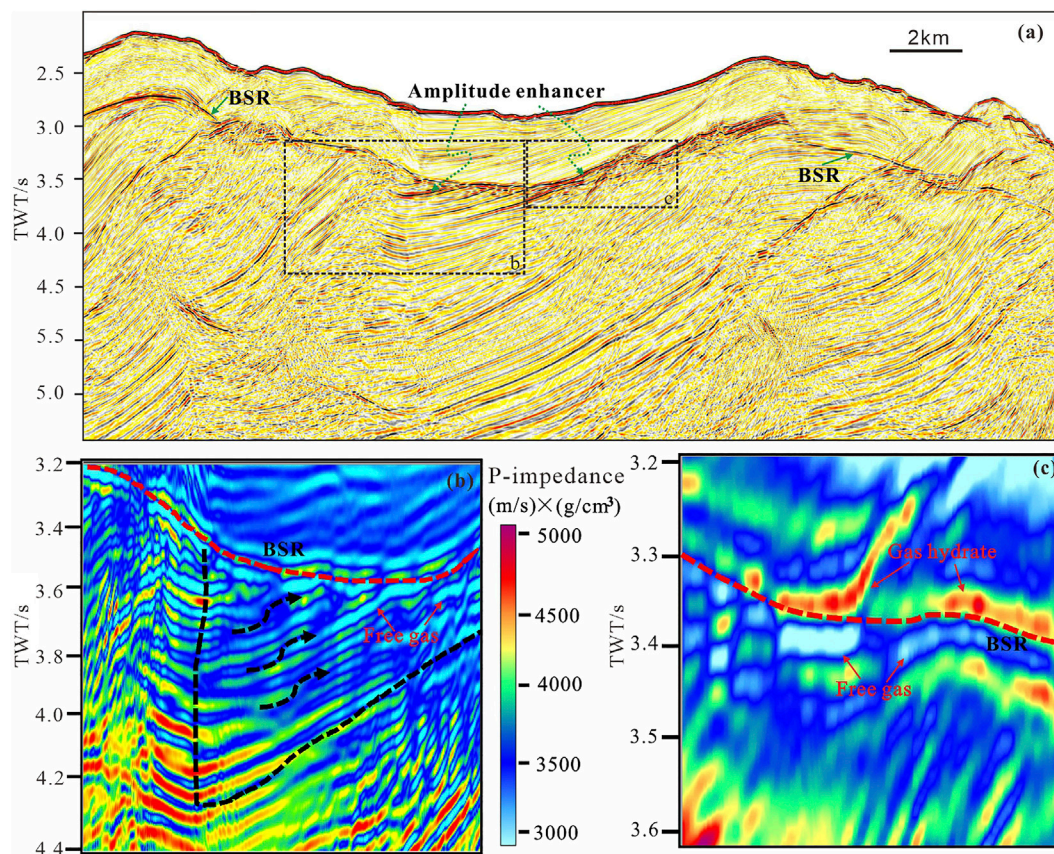


FIGURE 5 | Seismic profile (time domain) and detailed views of impedance inversion results (time domain). **(A)** Seismic profile; **(B)** impedance inversion results of the left part; **(C)** impedance inversion results of the right part.

present as amplitude-enhanced reflectors in the seismic profile (Figures 3, 5) and show high impedance anomalies in the impedance inversion profile (Figure 5). Seismic data interpretation and the analysis of sedimentary conditions indicate that deep hydrate reservoirs may consist of coarse-grained turbidites. Comprehensive analysis suggests that the strong amplitude and high impedance above the BSR in the study area probably indicate high saturation hydrate concentrated zones as well as coarse-grained sediments (Guo et al., 2017). By contrast, the strong amplitude and low impedance under the BSR reflect free gas concentrated zones (Figure 5). It should be noted that the piggyback basin under the BSR show the interbeds of slightly higher and low impedance, reflecting both the low impedance of free gas and the slightly higher impedance of turbidite sands.

3.2 Comparison of Characteristics of High Saturation Hydrate Reservoirs

3.2.1 Characteristics of Hydrate Reservoirs in the Nankai Trough, Japan

Two hydrate production tests have been conducted in 2012 in the Nankai Trough offshore Japan, which is a typical example of the

exploration and production tests of gas hydrates in active continental margins. According to Zhao, 2019, the high saturation hydrate reservoirs in the Nankai Trough were identified mainly based on the clear and continuous BSR, the existence of amplitude-enhanced reflectors above the BSR, high P-wave velocity, and sand-rich turbidites. The logging interpretation results show that the hydrates discovered in the first well (AT1-C) for coring and hydrate production tests in Japan are mainly concentrated in the wing of anticlinal ridges and show two layers of strong reflections above the BSR on the seismic profile (Figure 6) (Fujii et al., 2015). The upper layer of strong reflections is mainly composed of sheeted turbidite sands with high lateral continuity. By contrast, the lower layer of strong reflections consists of thick channel sands with poor lateral continuity, both sand layers have almost the same hydrate saturation of 50–80%. In addition, Komatsu et al. (2015) divided the 60 m thick hydrate concentrated zone of well AT1-C into four sedimentary facies zones based on logging curves (Figure 6). Analysis of sedimentary facies associations shows that the hydrate concentrated zone can be divided vertically into three portions, namely bottom turbidity channels, middle sheeted turbidity sands, and top basin-bottom sediments. Among them, the bottom and middle portions have the gas hydrates at the highest concentrated level (Ito et al., 2015).

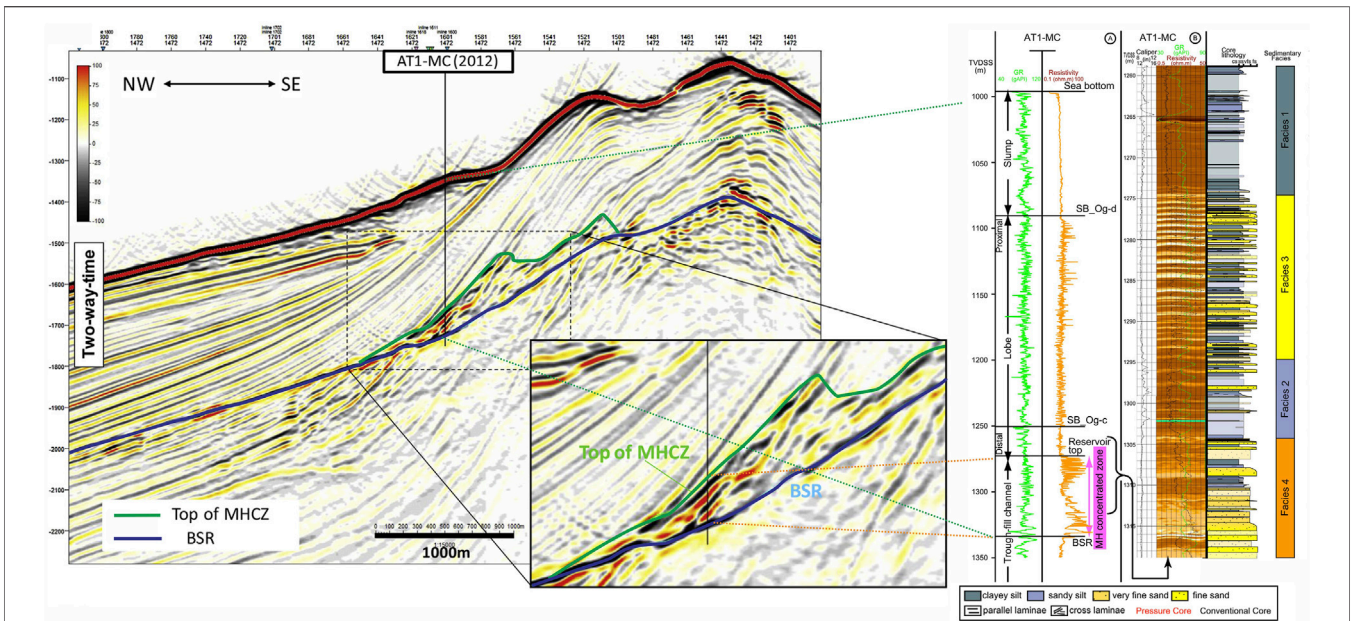


FIGURE 6 | Seismic reflection characteristics and sedimentary facies of high saturation hydrate deposits discovered during drilling in the Nankai Trough, Japan (Modified after Fujii et al., 2015; Komatsu et al., 2015). Note: High saturation hydrate deposits are located in the sand-rich turbidites with strong reflections above the BSR. MHCZ: methane hydrate concentrated zone.

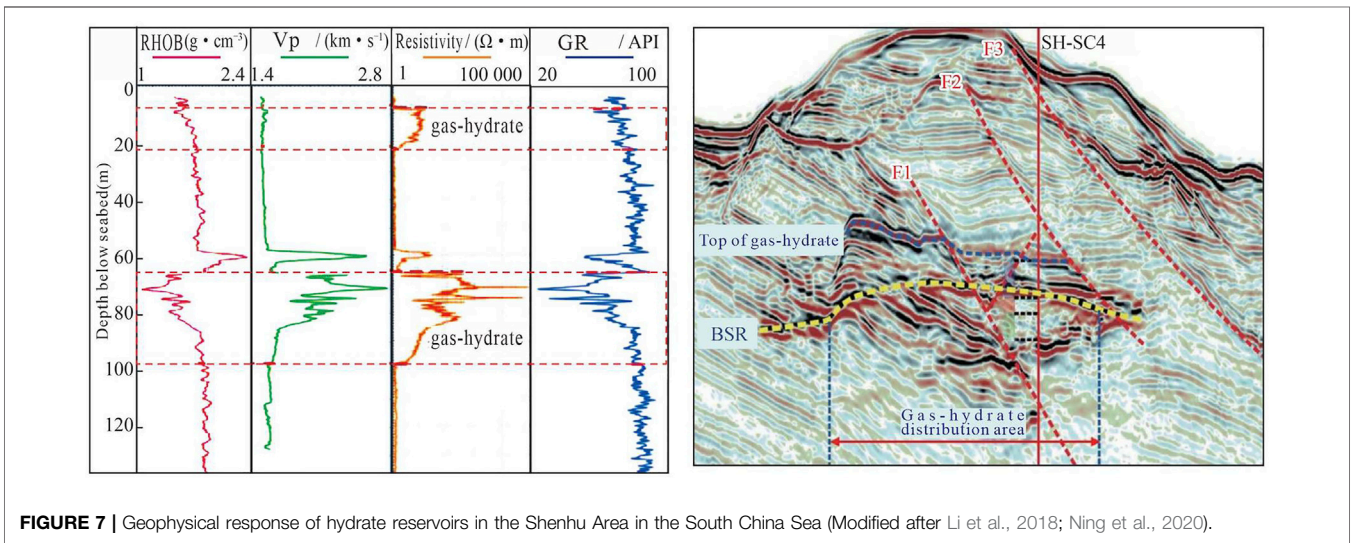


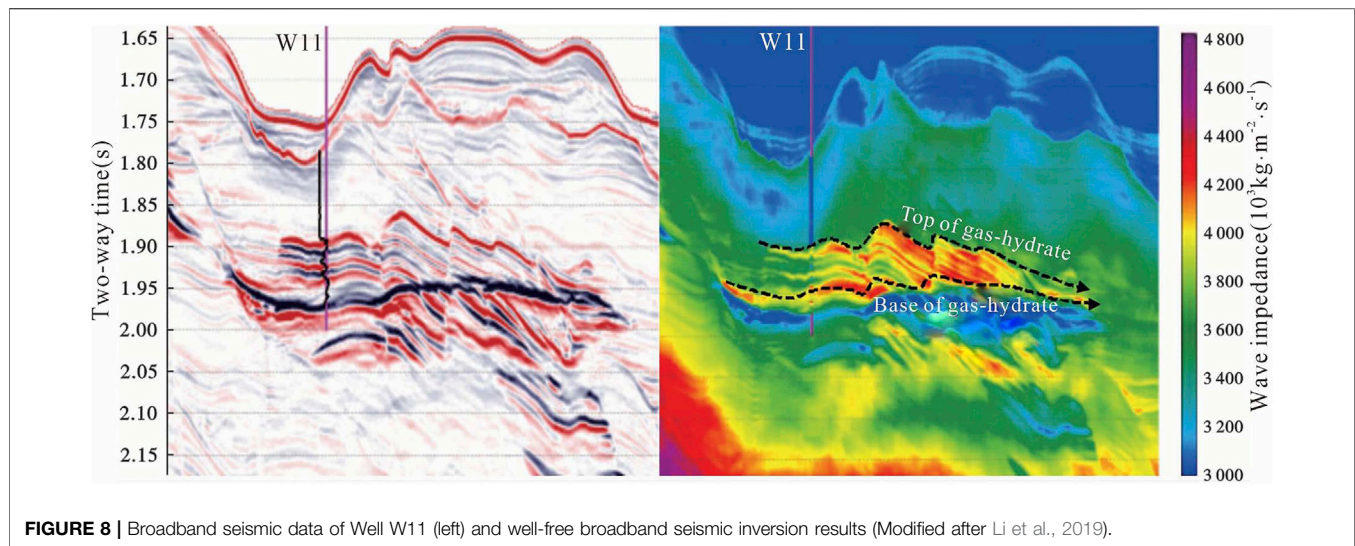
FIGURE 7 | Geophysical response of hydrate reservoirs in the Shenhu Area in the South China Sea (Modified after Li et al., 2018; Ning et al., 2020).

Therefore, the relatively continuous strong-amplitude reflections above the BSR indicate high-saturation hydrate deposits and highly permeable turbidites are high-saturation hydrate concentrated zones in the Nankai Trough.

3.2.2 Characteristics of Hydrate Reservoirs in the Shenhu Area, South China Sea

Three hydrate production tests have been conducted in the Shenhu Area in the South China Sea. Therefore, the Shenhu Area is also a model for the exploration and production tests

of gas hydrates of passive continental margins. According to comprehensive analyses (Zhang et al., 2014; Li et al., 2018; Su et al., 2020; Ning et al., 2020), the conditions for the concentration of high saturation hydrate deposits in the Shenhu Area are similar to those in the Nankai Trough, Japan (Figure 7), despite they are in different tectonic backgrounds. The logging curves show that the average P-wave velocity of hydrate concentrated zones in the Shenhu Area is about 2.03 km/s, while that of non-hydrate layers under the BSR is only 1.1–1.7 km/s (Ye et al., 2020).



In 2015, logging-while-drilling was conducted at 23 sites in the Shenhu Area carried out by the Guangzhou Marine Geological Survey. The logging data obtained during this expedition showed a hydrate saturation of up to 64%. Several sets of hydrate layers are vertically developed along Well W11, with a total thickness of over 70 m and a maximum hydrate saturation of up to 53%. By analyzing the seismic profile and synthetic seismic records of this well, Guo et al. (2017) found that the hydrate horizons are present as three strong reflections in the seismic profile and show strong impedance in the profile of synthetic seismic records. Li et al. (2019) obtained a detailed description of hydrate deposits passing through Well W11 using the well-free broadband seismic inversion technology (Figure 8). The inversion results clearly showed the top boundary, bottom boundary, and internal characteristics of the hydrate deposits in the Shenhu Area. Hydrate deposits in the Shenhu Area are located above the BSR and are manifested as three strong reflection axes (left, Figure 8), while the free gas under the BSR show weak impedance anomalies.

According to the above comparison, although there are different tectonic geological backgrounds, the corresponding relationship between strong reflection and gas hydrate is the same. We believe that the strong amplitude reflectors above BSR represents the existence of high saturation hydrate in both active and passive continental margins.

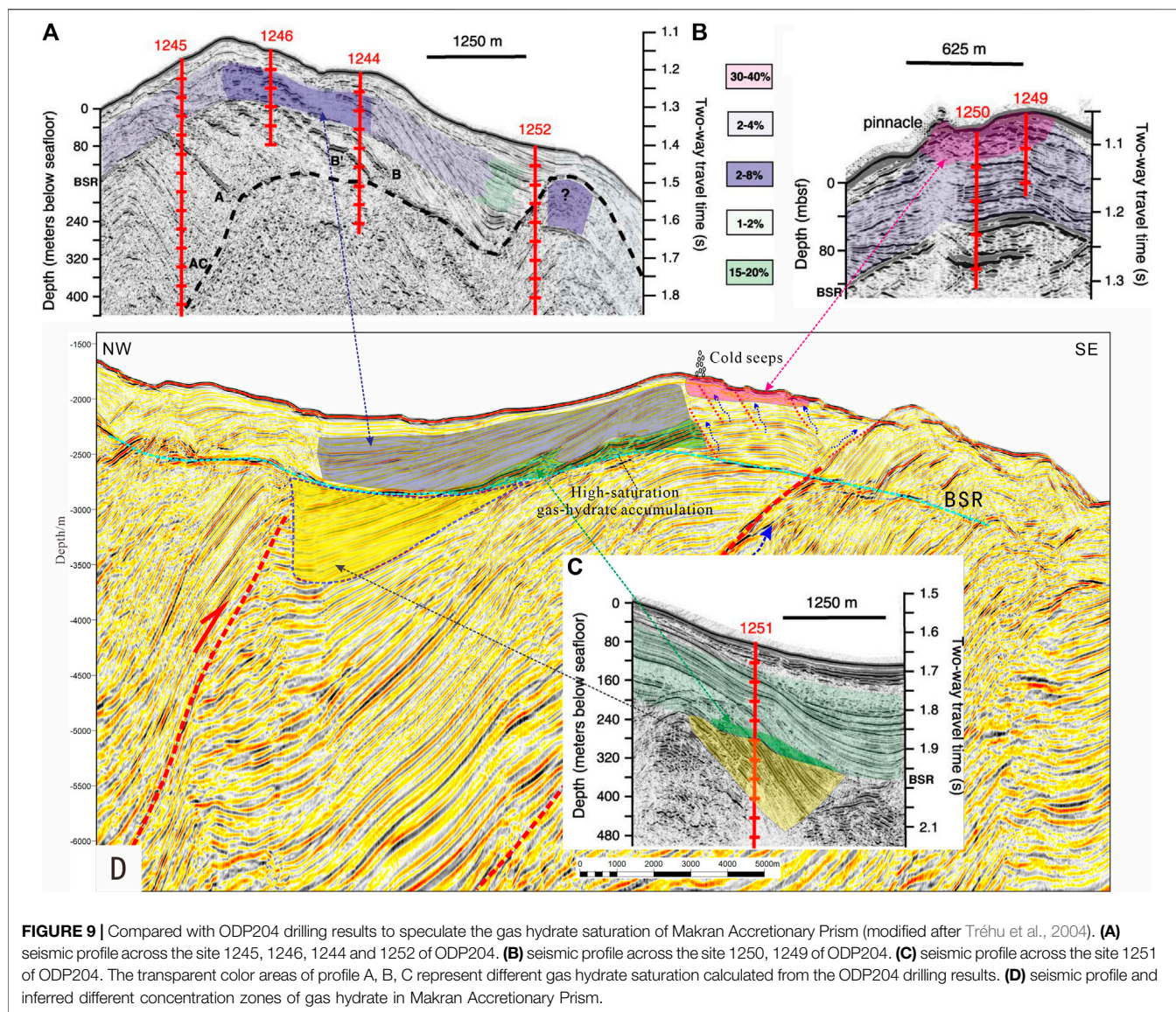
3.2.3 Analysis of Gas Hydrate Saturation by Comparison With ODP204

The seismic reflection characteristics of Makran Accretionary Prism are similar to those of Nankai Trough, and also can be compared with ODP204 drilling results (Tréhu et al., 2004). The drilling results of ODP204 show that gas hydrate is mainly distributed in three zones (Figure 9): 1. It is a high saturation accumulation area related to cold seeps, and its saturation can usually reach 30–40% (Figure 9B). The cold seep organisms found in the anticline ridge of Makran and the clear vertical channel on the seismic profile indicate that this type of hydrate distribution exists in the Makran area. However, its distribution range and thickness are

relatively small, and the amount of resources is relatively small; 2. The weak reflections between seafloor and BSR, which is thicker than the cold seeps zones, and the saturation is generally 2–8% (Figure 9A), but its distribution area is relatively large and its thickness is also large, so the amount of hydrate resources should be relatively large; 3. Strong reflection above BSR, with saturation of about 15–20% (Figure 9C), distribution zone between 1 and 2, thickness of about 100m, and contains large hydrate resources. In addition, it is strongly reflected under the BSR, which can be determined as free gas can be considered as a part of the gas hydrate system, with a thickness of up to 1000m, which contains a great amount of resources (Figure 9C).

3.3 Discussion of Characteristics of High Saturation Hydrate Reservoirs

- 1) Drilling results from the gas hydrate reservoirs in the Nankai Trough, Japan confirmed that the amplitude-enhanced reflectors above the BSR are high saturation hydrate concentrated zones and that aquifers lacking amplitude-enhanced reflectors exist under the BSR. According to the logging curves of the gas hydrate reservoirs in the Nankai Trough, the sedimentary strata under the BSR show low resistivity and high gamma ray intensity (Figure 6). This indicates that the content of argillaceous materials increases and that the storage space decreases under the BSR accordingly. These conditions are unfavorable for the accumulation of free gas.
- 2) Drilling and impedance inversion results from the gas hydrate reservoirs in the Shenhu Area show that amplitude-enhanced reflectors coexisting with high impedance anomalies above the BSR are also high saturation hydrate concentrated zones. By contrast, the amplitude-enhanced reflectors below the BSR show low resistivity, high gamma ray intensity, and low impedance (Figures 7, 8). Therefore, it can be inferred that the free gas under the BSR has low saturation.
- 3) The results of seismic interpretation and wave impedance inversion from the hydrate reservoirs in the Makran



Accretionary Prism indicate that amplitude-enhanced reflectors exist in the anticline wing above the BSR and the syncline area of the piggyback basin under the BSR. Given these results and the comparative analysis of characteristics of hydrate reservoirs in the Nankai Trough and the Shenhu Area, it can be inferred that the amplitude-enhanced reflectors above the BSR that coexist with high impedance anomalies are possibly high saturation hydrate concentrated zones.

- 4) The amplitude-enhanced reflectors below the BSR in the hydrate reservoirs in the Makran Accretionary Prism may be free gas concentrated zones. The slightly higher impedance anomalies coexisting with the amplitude-enhanced reflectors are related to the distribution state of the free gas in the strata or the coexistence of free gas and hydrates. In fact, the free gas below the BSR in the study area primarily occurs in coarse-grained turbidite sand

layers and constitutes oblique interlayers together with mud layers. Such inclined layered distribution of free gas will change the velocity of gas-bearing sediments (Ojha and Sain, 2008). In addition, transition zones consisting of hydrates, free gas, and water exist below the hydrate deposits in the areas of production tests in the Shenhu Area (Qin et al., 2020). The degree of mixing of the substances of different phases in the transition zones changes the velocity of gas-bearing sediments, for which the specific reasons require further investigation.

4 CONCLUSION

- 1) According to the comprehensive analyses, the conditions for the formation of high saturation hydrate reservoirs should be characterized by a clear and continuous BSR, the coexistence

of amplitude-enhanced reflectors and high impedance anomalies above the BSR, high P-wave velocity, and relatively coarse-grained sediments.

- 2) The Makran Accretionary Prism has thick sediments, developed transport systems of “two-way gas supply” (i.e., thrust fault and normal fault, thrust fault and high permeable strata), and a clear and continuous BSR. Meanwhile, apparent amplitude-enhanced reflectors exist above and below the BSR. According to the impedance inversion results, the anticline wings above the BSR and the syncline area of the piggyback basin below the BSR show strong and a little strong impedance anomalies, respectively.
- 3) As inferred from the drilling results of high saturation hydrate reservoirs in the world, high saturation hydrate reservoirs in the Makran Accretionary Prism are mainly probably distributed in the anticline wings immediately above the BSR. Moreover, these reservoirs are characterized by coarse-grained sediments and the coexistence of amplitude-enhanced reflectors and high impedance anomalies.
- 4) The saturation of gas hydrate near cold seeps can reach 30–40%. However, its distribution range and thickness are relatively small, and the resources is relatively small. The saturation of gas hydrate of weak reflections between seafloor and BSR is generally 2–8%, the amount of hydrate resources should be relatively large. Strong reflection above BSR, with saturation of about 15–20% contains large hydrate resources. The free gas under the BSR with a thickness of up to 1000 m contains a great amount of gas.

DATA AVAILABILITY STATEMENT

The raw data supporting the conclusions of this article will be made available by the authors, without undue reservation.

REFERENCES

- Baba, K., and Yamada, Y. (2004). BSRs and Associated Reflections as an Indicator of Gas Hydrate and Free Gas Accumulation: an Example of Accretionary Prism and Forearc basin System along the Nankai Trough, off central Japan. *Resource Geology*. 54, 11–24. doi:10.1111/j.1751-3928.2004.tb00183.x
- Bohrmann, G., and Ohling, G. (2008). *Cold Seeps of the Makran Subduction Zone (Continental Margin of Pakistan): R/V Meteor Cruise Report M74/3:M74, Leg3, Fujairah-Male 30 October-28 November, 2007*. Fachbereich Geowissenschaften, Universität Bremen, 1–120.
- Delisle, G. (2004). The Mud Volcanoes of Pakistan. *Env Geol*. 46, 1024–1029. doi:10.1007/s00254-004-1089-x
- Delisle, G., von Rad, U., Andruleit, H., Von Daniels, C., Tabrez, A., and Inam, A. (2002). Active Mud Volcanoes on- and Offshore Eastern Makran, Pakistan. *Int. J. Earth Sci.* 91, 93–110. doi:10.1007/s005310100203
- Fujii, T., Suzuki, K., Takayama, T., Tamaki, M., Komatsu, Y., Konno, Y., et al. (2015). Geological Setting and Characterization of a Methane Hydrate Reservoir Distributed at the First Offshore Production Test Site on the Daini-Atsumi Knoll in the Eastern Nankai Trough, Japan. *Mar. Pet. Geology*. 66, 310–322. doi:10.1016/j.marpetgeo.2015.02.037

AUTHOR CONTRIBUTIONS

JL is responsible for the interpretation of seismic data and compilation of the paper; XL is responsible for the inversion of gas hydrate seismic data; ZQ is responsible for the comparison of the characteristics of gas hydrate deposits with high saturation, JG is responsible for the analysis of the characteristics of gas hydrate deposits, WY is responsible for the collection of gas hydrate deposits in the Nankai Trough, SL, BL and JL are responsible for collecting the accumulation conditions of the gas hydrate deposits in the Shenhu area, KM and SW are responsible for collecting the relevant data on the accretion prism gas hydrate offshore Makran.

FUNDING

This study was funded by Marine S&T Fund of Shandong Province for Pilot National Laboratory for Marine Science and Technology (Qingdao) (2021QNLM020001-1) and the National Natural Science Foundation projects of China (42076069, 41706072), China Geological Survey project (DD20190581).

ACKNOWLEDGMENTS

The authors would like to express their gratitude to all members of R/V Haiyangdizhi 9, who assisted in the collection of field data for this project. Thanks also go to the reviewers and editors of this manuscript for their suggestions.

SUPPLEMENTARY MATERIAL

The Supplementary Material for this article can be found online at: <https://www.frontiersin.org/articles/10.3389/feart.2022.861162/full#supplementary-material>

- Gong, J. M., Liao, J., Sun, J., Yang, C. S., Wang, J. Q., He, Y. J., et al. (2016). Main Controlling Factors of Natural Gas Hydrate in Makran Accretionary Prism Pakistan. *Mar. Geology. Frontier* 32, 10–15. (in Chinese with English abstract).
- Gong, J. M., Liao, J., Yang, C. S., Cheng, H. Y., Sun, J., Wang, J. Q., et al. (2017). The Relationship between Authigenic Carbonate and Gas Hydrates in Makran Accretionary Wedge: on the Basis of M 74/3 Cruise Report of "R/V Meteor" in 2007. *Mar. Geology. Front.* 33, 20–26. (in Chinese with English abstract).
- Gong, J. M., Liao, J., Yin, W. H., Zhang, L., He, Y. J., Sun, Z. L., et al. (2018a). Gas Hydrate Accumulation Models of Makran Accretionary Prism, Northern Indian Ocean. *Mar. Geology. Quat. Geology*. 38, 148–155. (in Chinese with English abstract).
- Gong, J. M., Liao, J., Zhang, L., He, Y. J., Zhai, B., Meng, M., et al. (2018b). Discussion on the Distribution and Main Controlling Factors of Mud Volcanoes in Makran Accretionary prism, Northern Indian Ocean. *Geoscience* 32, 1025–1030. (in Chinese with English abstract).
- Grando, G., and McClay, K. (2007). Morphotectonics Domains and Structural Styles in the Makran Accretionary Prism, Offshore Iran. *Sediment. Geology*. 196, 157–179. doi:10.1016/j.sedgeo.2006.05.030
- Grevemeyer, I., Rosenberger, A., and Villingger, H. (2000). Natural Gas Hydrates on the continental Slope off Pakistan: Constraints from Seismic Techniques. *Geophys. J. Int.* 140, 295–310. doi:10.1046/j.1365-246x.2000.00009.x

- Guo, Y. Q., Yang, S. X., Liang, J. Q., Lu, J. A., Lin, L., and Kuang, Z. G. (2017). Characteristics of High Gas Hydrate Distribution in the Shenhu Area on the Northern Slope of the South China Sea. *Earth Sci. Front.* 24, 24–31. (in Chinese with English abstract).
- Hu, G. W., Bu, Q. T., Lu, W. J., Wang, J. S., Chen, J., Li, Q., et al. (2020). A Comparative Study on Natural Gas Hydrate Accumulation Models at Active and Passive continental Margins. *Nat. Gas Industry* 40, 45–58.
- Hussain, A., Khan, M. R., Ahmad, N., and Javed, T. (2015). *Mud-diapirism Induced Structuration and Implications for the Definition and Mapping of Hydrocarbon Traps in Makran Accretionary Prism*. Melbourne, Australia: Pakistan//AAPG/SEG International Conference&Exhibition, 13–16.
- Hyndman, R., and Spence, G. (1992). A Seismic Study of Methane Hydrate marine Bottom Simulation Reflectors. *Geophys. Res.* 97, 6638–6698. doi:10.1029/92jb00234
- Ito, T., Komatsu, Y., Fujii, T., Suzuki, K., Egawa, K., Nakatsuka, Y., et al. (2015). Lithological Features of Hydrate-Bearing Sediments and Their Relationship with Gas Hydrate Saturation in the Eastern Nankai Trough, Japan. *Mar. Pet. Geology*. 66, 368–378. doi:10.1016/j.marpetgeo.2015.02.022
- Komatsu, Y., Suzuki, K., and Fujii, T. (2015). Sedimentary Facies and Paleoenvironments of a Gas-Hydrate-Bearing Sediment Core in the Eastern Nankai Trough, Japan. *Mar. Pet. Geology*. 66, 358–367. doi:10.1016/j.marpetgeo.2015.02.038
- Kopp, C., Fruehn, J., Flueh, E. R., Reichert, C., Kukowski, N., Bialas, J., et al. (2000). Structure of the Makran Subduction Zone from Wide-Angle and Reflection Seismic Data. *Tectonophysics* 329, 171–191. doi:10.1016/s0040-1951(00)00195-5
- Li, J.-f., Ye, J. L., Ye, J.-l., Qin, X.-w., Qiu, H.-j., Wu, N.-y., et al. (2018). The First Offshore Natural Gas Hydrate Production Test in South China Sea. *China Geology*. 1, 5–16. doi:10.31035/cg2018003
- Li, Y. P., Yan, C. Z., Li, J., Shi, W. Y., and Chen, L. (2019). Application of Well-free Broadband Seismic Inversion Technology on the Description of Gas Hydrate Ore Body in Shenhu Waters, South China Sea. *China Offshore Oil and Gas* 31, 51–60. (in Chinese with English abstract).
- Liao, J., Gong, J. M., He, Y. J., Yue, B. J., and Meng, M. (2019). Stratigraphic Sequence and Development Process of Makran Accretionary Prism. *Mar. Geology. Frontier* 35, 69–72. (in Chinese with English abstract).
- Ning, F. L., Liang, J. Q., Wu, N. Y., Zhu, Y. H., Wu, S. G., Liu, C. L., et al. (2020). Reservoir Characteristics of Natural Gas Hydrates in China. *Nat. Gas Industry* 40, 1–24. (in Chinese with English abstract).
- Ojha, M., and Sain, K. (2008). Appraisal of Gas-Hydrate/free-Gas from Vp/Vs Ratio in the Makran Accretionary Prism. *Mar. Pet. Geology*. 25, 637–644. doi:10.1016/j.marpetgeo.2007.10.007
- Qin, X. W., Lu, J. A., Lu, H. L., Qiu, H. J., Liang, J. Q., Kang, D. J., et al. (2020). Coexistence of Natural Gas Hydrate, Free Gas and Water in the Gas Hydrate System in the Shenhu Area, South China Sea. *China Geology*. 2, 210–220.
- Riedel, M., Collett, T. S., and Malone, M. J. (2010). *Expedition 311 Synthesis: Scientific findings//Proceedings of the Integrated Ocean Drilling Program*, 311. Washington, DC: Integrated Ocean Drilling Program Management International Inc.
- Riedel, M., and Shankar, U. (2012). Combining Impedance Inversion and Seismic Similarity for Robust Gas Hydrate Concentration Assessments-A Case Study from the Krishna-Godavari basin. *East. Coast India Mar. Pet. Geology*. 36, 35–49. doi:10.1016/j.marpetgeo.2012.06.006
- Riedel, M., Willoughby, E. C., and Chopra, S. (2010). *Geophysical Characterization of Gas Hydrate*, 14. USA: SEG Geophysical Developments.
- Sain, K., Minshull, T. A., Singh, S. C., and Hobbs, R. W. (2000). Evidence for a Thick Free Gas Layer beneath the Bottom Simulating Reflector in the Makran Accretionary Prism. *Mar. Geology*. 164, 3–12. doi:10.1016/s0025-3227(99)00122-x
- Smith, G. L. (2013). *The Structure, Fluid Distribution and Earthquake Potential of the Makran Subduction Zone, Pakistan*. Southampton: Great Britain University of Southampton.
- Su, P. B., Liang, J. Q., Zhang, W., Liu, F., Wang, F. F., Li, T. W., et al. (2020). Natural Gas Hydrate Accumulation System in the Shenhu Sea Area of the Northern South China Sea. *Nat. Gas Industry* 40, 77–89.
- Tréhu, A. M., Long, P. E., Torres, M. E., Bohrmann, G., Rack, F. R., Collett, T. S., et al. (2004). Three-Dimensional Distribution of Gas Hydrate beneath Southern Hydrate Ridge: Constraints from ODP Leg 204. *Earth Planet. Sci. Lett.* 222 (3–4), 845–862.
- Von Rad, U., Berner, U., Delisle, G., Dooze-Rolinski, H., Fechner, N., Linke, P., et al. (2000). Sonne 122/130 Scientific Parties Gas and Fluid Venting at the Makran Accretionary Prism off Pakistan. *Geo-Marine Lett.* 20, 10–19. doi:10.1007/s003670000033
- Wan, X. M., Liang, J., Liang, J. Q., Lin, L., Sha, Z. B., Chai, Y., et al. (2016). The Application of post-stack Impedance Inversion without Well to the Prediction of Gas Hydrate Distribution in T Study Area. *Geophys. Geochemical Exploration* 40, 438–444. (in Chinese with English abstract).
- Xue, H., Zhang, B. J., Xu, Y. X., Wen, P. F., and Zhang, R. W. (2016). Application of Wave Impedance Inversion to Gas Hydrates Prediction in Southeast Hainan basin. *Mar. Geology. Quat. Geology*. 36, 173–180. (in Chinese with English abstract).
- Ye, J. L., Qin, X. W., Xie, W. W., Lu, H. L., Ma, B. J., Qiu, H. J., et al. (2020). Main Progress of the Second Gas Hydrate Trial Production in the South China Sea. *Geology. China* 47, 557–568. (in Chinese with English abstract).
- Zhang, G. X., Liang, J. Q., Lu, J. Q., Yang, J. G., Lu, J. A., Yang, S. X., et al. (2014). Characteristics of Natural Gas Hydrate Reservoirs on the Northeastern Slope of the South China Sea. *Nat. Gas Industry* 34, 1–10. (in Chinese with English abstract).
- Zhang, G. X., Zhu, Y. H., Liang, J. Q., Wu, S. G., Yang, M. Z., and Sha, Z. B. (2006). Tectonic Controls on Gas Hydrate Deposits and Their Characteristics. *Geoscience* 20, 605–612.
- Zhang, Z., He, G. W., Yao, H. Q., Deng, X. G., Yu, M., Huang, W., et al. (2020). Diapir Structure and its Constraint on Gas Hydrate Accumulation in the Makran Accretionary Prism, Offshore Pakistan. *China Geology*. 3, 611–622. doi:10.31035/cg2020049
- Zhao, K. B. (2019). Occurrence and Accumulation Characteristics of Natural Gas Hydrate in the Eastern Nankai Trough, Japan. *Pet. Geology. Exp.* 41, 831–837. (in Chinese with English abstract).

Conflict of Interest: The authors declare that the research was conducted in the absence of any commercial or financial relationships that could be construed as a potential conflict of interest.

Publisher's Note: All claims expressed in this article are solely those of the authors and do not necessarily represent those of their affiliated organizations, or those of the publisher, the editors and the reviewers. Any product that may be evaluated in this article, or claim that may be made by its manufacturer, is not guaranteed or endorsed by the publisher.

Copyright © 2022 Liao, Liu, Zhao, Gong, Yin, Li, Lei, Liang, Muhammad and Syed. This is an open-access article distributed under the terms of the Creative Commons Attribution License (CC BY). The use, distribution or reproduction in other forums is permitted, provided the original author(s) and the copyright owner(s) are credited and that the original publication in this journal is cited, in accordance with accepted academic practice. No use, distribution or reproduction is permitted which does not comply with these terms.